Available online at www.sciencedirect.com

ScienceDirect

Ceramics International 39 (2013) 8911–8916

CERAMICS INTERNATIONAL

www.elsevier.com/locate/ceramint

Efficient near-infrared to visible and ultraviolet upconversion in polycrystalline BiOCl:Er^{3+}/Yb^{3+} synthesized at low temperature

Yongjin Li[a], Zhiguo Song[a,b,*], Chen Li[a], Ronghua Wan[a], Jianbei Qiu[a,b], Zhengwen Yang[a,b], Zhaoyi Yin[a,b], Yong Yang[a,b], Xue Wang[a], Qi Wang[a]

[a]*School of Materials Science and Engineering, Kunming University of Science and Technology, Xuefu Road, Kunming 650093, China*
[b]*Key Lab of Advanced Materials in Rare and Precious and nonferrous Metals (Kunming University of Science and Technology), Ministry of Education, Xuefu Road, Kunming 650093, China*

Received 23 January 2013; received in revised form 8 April 2013; accepted 24 April 2013
Available online 1 May 2013

Abstract

Er^{3+}/Yb^{3+} co-doped BiOCl poly-crystals were synthesized by the conventional solid state method at 500 °C, which exhibited good crystalline and low phonon energy. Under 980 nm excitation, the samples showed intense red upconversion (UC) luminescence (Er^{3+}: $^4F_{9/2} \rightarrow {}^4I_{15/2}$) as well as other four UC emission bands, including ultraviolet (UV) emission at 380 nm, violet emission at 411 nm, green UC emissions at 525 and 545 nm and near-infrared (NIR) emission between 800 and 850 nm, corresponding to the transitions of $^4G_{11/2}$, $^2H_{9/2}$, $^2H_{11/2}$, $^4S_{3/2}$ and $^4I_{9/2} \rightarrow {}^4I_{15/2}$ of Er^{3+}, respectively. Interestingly, including the violet and green UC emissions, the red one originated a nearly three-photon process in this system, and a possible UC mechanism was proposed for the enhanced red emission.

Keywords: Er^{3+}/Yb^{3+}; BiOCl; Upconversion

1. Introduction

Upconversion (UC) of near infrared (NIR) light into visible and ultraviolet (UV) light by lanthanide (Ln)-doped materials has attracted much more attention in the present days due to the possibility of infrared pumped visible eye-safe lasers and their potential applications, such as three-dimensional display, optical data storage, optoelectronics, medical diagnostics, sensors, and undersea optical communication [1–6]. The UC process involves rare earth (RE) ions in a host lattice, where single or multi-photon excitation of electrons leads to the subsequent emission of photons at higher energies [7]. In order to fulfill the corresponding requirements in various application fields, the selection of the host is an important factor to obtain highly efficient UC luminescence. Besides low phonon energy of the host materials that can result in a reduction of the multi-phonon relaxation thus helps efficient UC occur [8], the different crystal fields caused by structural symmetry of the host materials can also contribute to inner shell transitions such as intra 4f–4f transitions in RE ions [9]. In recent years, for the host of UC materials, much attention has been focused on fluoride compounds for lower phonon energies and rare earth oxides due to better chemical stability and mechanical strength [10–12]. In fact, both their production costs are high, restricting their use in practical application.

BiOCl is a type of wide band gap semiconductor material with a band gap of 3.5 eV, which have a tetragonal *PbFCl* type with a space group of *P4/nmm* [13]. During the past few years, BiOCl has drawn considerable attention for industrial applications, such as, photo-catalysts, magnetic materials because of their unique electronic structure and catalytic performance [14–16]. However, its luminescence properties were seldom reported [17,18]. In facts, host materials with a wide band gap are attractive for optical applications in the visible and UV spectral ranges, because the rare earths can emit within its optical window and do not suffer from quenching effects

*Corresponding author at: School of Materials Science and Engineering, Kunming University of Science and Technology, Xuefu Road, Kunming 650093, China. Tel./fax: +86 871 518 8856.
E-mail addresses: songzg@kmust.edu.cn, blackysong@yahoo.com.cn (Z. Song).

0272-8842/$ - see front matter © 2013 Elsevier Ltd and Techna Group S.r.l. All rights reserved.
http://dx.doi.org/10.1016/j.ceramint.2013.04.085

inherent to semiconductor hosts [19,20]. On the other hand, different with rare earth oxychloride, such as YOCl, GdOCl, etc. [21,22], whose valence band energy levels are due predominantly to the O-2p and Cl-3p orbitals, whereas in Bi crystals, because of particular electronic structure, the top of the valence band would be composed of the mixture O-2p, Cl-3p, Bi-6s and Bi-6p orbitals, and the Bi-6p orbitals dominate the conduction band [23,24]. Therefore, Bi could be a more favorable cation than Y and Gd for RE^{3+} ions dopant emission [25]. We expect that BiOCl could act as an efficient host for UC luminescence. Importantly, BiOCl possesses facile synthesis of crystallized form by solid reactions with low temperature calcinations, which can be produced at a low cost.

In this work, we synthesized Er^{3+}/Yb^{3+} co-doped BiOCl power by the conventional solid state method at a mild temperature. Efficient NIR to UV UC luminescence in Er^{3+}/Yb^{3+} co-doped BiOCl were realized under 980 nm excitation. As the Er^{3+} or Yb^{3+} ions concentrations increase, the intensity of overall UC luminescence increases at first then decreases. Importantly, it was found that the violet, green and red UC emission mainly resulted from three-photon excitation, and the reasons as well as the possible UC mechanism were discussed.

2. Experimental

The Er^{3+}/Yb^{3+} co-doped BiOCl powders were synthesized by the traditional solid state reaction. NH_4Cl (A.R., Tianjin, China), Bi_2O_3 (99.99%, Sichuan, China), Yb_2O_3 (99.99%, Shanghai, China) and Er_2O_3 (99.99%, Shanghai, China) were used as the starting materials. The mixture ratio of the reactants was: $Bi_{(1-0.05-x)}Yb_{0.05}Er_xOCl$ ($x=1$, 2, 3, 4 mol%) and $Bi_{(1-0.02-y)}Yb_yEr_{0.02}OCl$ ($y=0$, 1, 2.5, 5, 7.5, 10, 15 mol%). The weighed raw materials were thoroughly mixed in an agate mortar and then placed in a corundum crucible. Then, the powders were sintered at 500 °C for 3 h in air. It should be noticed that NH_4Cl were added in excess of 20% to supply the chlorine rich atmosphere during the sintering process in order to compensate for volatilization losses. For comparison, the un-doped BiOCl was prepared by the same procedure, using starting materials of NH_4Cl and Bi_2O_3.

The crystalline structure of samples was characterized by powder X-ray diffraction (XRD) (Bruker D8-Advance diffractometer using Cu $K\alpha$ ($\lambda=1.5406$ Å) radiation). Raman spectra were performed by using Micro-Raman Spectroscopy System (Renishaw invia). A 980 nm continuous wave diode laser was used as the excitation source, and the UC and down-conversion luminescence spectra of the sample were measured using the Hitachi F-7000 Fluorescence Spectrophotometer. All measurements were made at room temperature.

3. Results and discussion

The XRD patterns of Er^{3+}/Yb^{3+} co-doped BiOCl displays that all of the XRD peaks could be indexed to the tetragonal structure of BiOCl with space group of *P4/nmm* (JCPDS: No.06-0249) (Fig. 1(a)). No other impurity peak was observed, indicating that pure phase Er^{3+}/Yb^{3+} co-doped BiOCl crystals are successfully

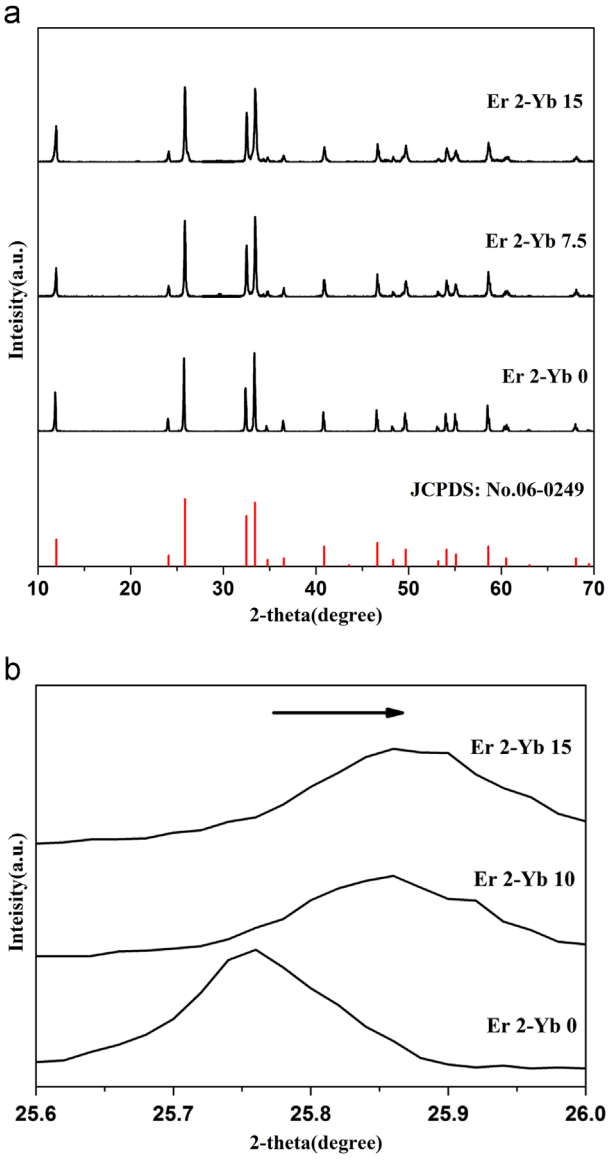

Fig. 1. XRD patterns of BiOCl power with (a) Er^{3+} concentration of 2 mol% and Yb^{3+} concentration of 0,7.5,15 mol%. (b) The main diffraction peak near $2\theta=25.75°$ with increasing Yb^{3+} concentration.

synthesized at such a low temperature. It is noteworthy that the diffraction peaks shift to high 2θ angles and become broad with increasing Yb^{3+} ion dopants, as showed in Fig. 1(b). Moreover, according to Scherer's Equation [26] and the equation below:

$$1/d^2 = (h^2 + k^2)/a^2 + l^2/c^2 \quad (1)$$

where d, a, c and (h k l) are the diffraction distance, lattice constant and crystal indices (Miller indices), respectively, the crystallite sizes and lattice constants were calculated and shown in Table 1. It shows that the crystallite sizes and lattice constants of BiOCl decrease as the concentration of Yb^{3+} ions increases. Considering the facts that the ion radius of Er^{3+} and Yb^{3+} are smaller than that of Bi^{3+}, the XRD results demonstrate that Er^{3+} and Yb^{3+} ions are effectively doped into the host lattice.

Table 1
Calculated crystallite sizes and lattice constants of Er^{3+}/Yb^{3+} co-doped BiOCl.

Yb^{3+} concentration (mol%)	Crystallite size (nm)	Lattice constant (Å)	
		a	*c*
0	79.6	3.9044	7.4477
7.5	62.4	3.8957	7.3953
15	57.5	3.8953	7.3868

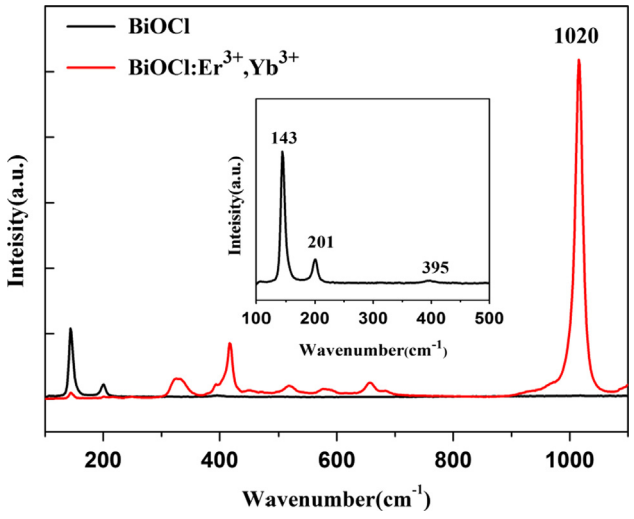

Fig. 2. Raman spectra of BiOCl and Er^{3+}/Yb^{3+} co-doped BiOCl power at room temperature.

Fig. 2 shows the Raman spectrum of obtained un-doped BiOCl and Er^{3+}/Yb^{3+} co-doped BiOCl power. The sample presents the characteristic vibration modes of BiOCl, which are located at 143, 201 and 395 cm^{-1}. The band at 143 cm^{-1} is ascribed to the A_{1g} internal Bi-Cl stretching mode and the band at 201 cm^{-1} is assigned to the E_g internal Bi–Cl stretching modem. In addition, the weak band at 395 cm^{-1} is assigned to the E_g and B_{1g} modes involving the motion of the oxygen atoms [15]. Because the host material with low phonon energies is very beneficial for getting high UC efficiency, as we supposed, BiOCl is a potentially efficient host material for UC luminescence. Moreover, it shows that the co-doping of Er^{3+} and Yb^{3+} ion results in a new vibration band peaked at 1020 cm^{-1}, which is probably due to the different local vibration modes of lanthanide impurities and may have influence on the UC luminescence properties.

Upon excitation at 980 nm, the Er^{3+}/Yb^{3+} co-doped BiOCl crystals exhibit efficient NIR to UV UC luminescence (Fig. 3). The UC luminescence spectra are consisted of five regions: (1) the much weaker UV emission centered at about 380 nm is attributed to the $^4G_{11/2}\rightarrow{}^4I_{15/2}$ transition, (2) the weak violet emission peak at 411 nm is duo to the $^2H_{9/2}\rightarrow{}^4I_{15/2}$ transition, (3) the green emission centered at about 525 and 545 nm are attributed to the $^2H_{11/2}$, $^4S_{3/2}\rightarrow{}^4I_{15/2}$, (4) very strong red emission between 640 and 710 nm, corresponding to the $^4F_{9/2}\rightarrow{}^4I_{15/2}$ transitions and (5) the NIR emission between 800 and 850 nm are attributed to the $^4I_{9/2}\rightarrow{}^4I_{15/2}$ of Er^{3+} ions, respectively.

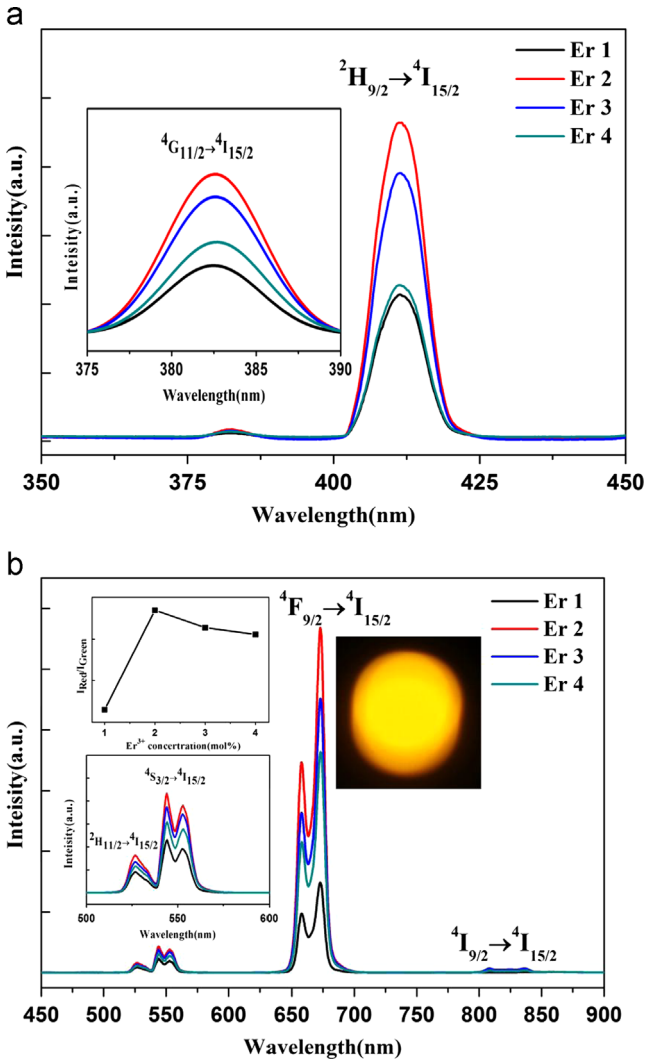

Fig. 3. UC spectra of Er^{3+}/Yb^{3+} co-doped BiOCl under the excitation of 980 nm with constant Yb^{3+} concentrations (5 mol%) and different Er^{3+} ion concentrations (from 1 to 4 mol%). The inset is the red/green ratio as a function of Er^{3+} concentrations and the luminescent photograph of Er^{3+}/Yb^{3+} (2/5 mol%) co-doped BiOCl under the excitation of 980 nm at 1.5 W. (For interpretation of the references to color in this figure legend, the reader is referred to the web version of this article.)

In order to study and optimize the UC luminescence properties of Er^{3+}/Yb^{3+} co-doped BiOCl, effects of Er^{3+} and Yb^{3+} concentrations on the UC emissions were investigated and shown in Figs. 3 and 4, respectively. Fig. 3 presents the UC emission spectra of the samples doped with constant Yb^{3+} ions (5 mol%) and different Er^{3+} ion concentrations (from 1 to 4 mol%). It shows that overall emission intensity as well as the intensity ratio of red to green emission increases as Er^{3+} ions concentration increases from 1 to 2 mol%, especially for the red emission, and then decrease due to concentration quenching effect [9]. On the other hand, the relative intensity ratio of red emission to green one shows little change when the Er^{3+} ions concentration is upon 2 mol%, and as a result the samples exhibit bright yellow luminescence (inset of Fig. 3(b)).

Fig. 4 shows the UC emission spectra for constant Er^{3+} concentrations (2 mol%) and different Yb^{3+} ion concentrations

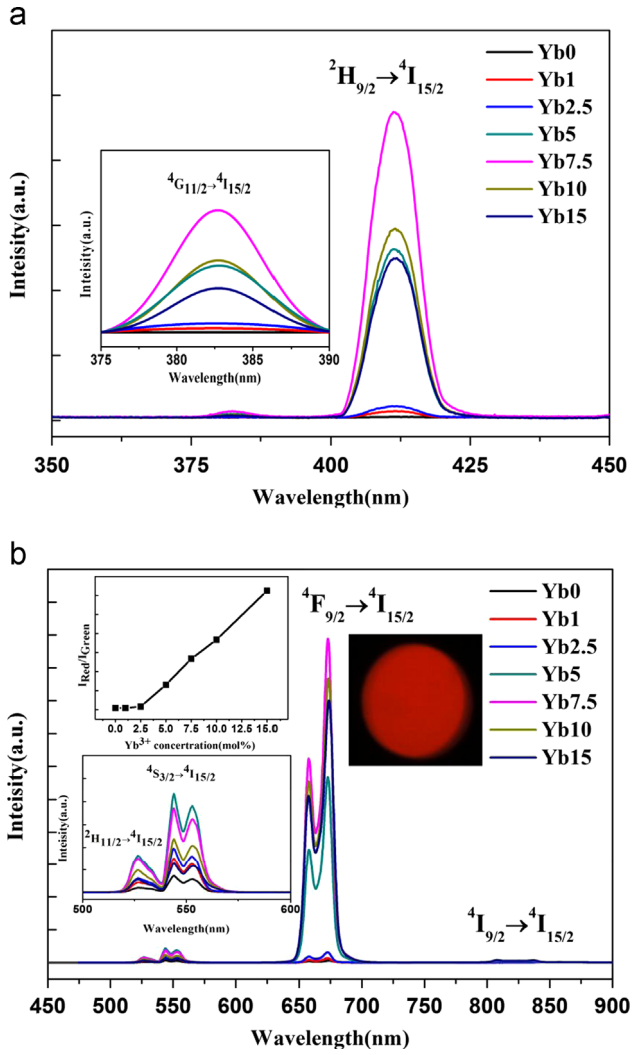

Fig. 4. UC spectra of Er^{3+}/Yb^{3+} co-doped BiOCl under the excitation of 980 nm with constant Er^{3+} concentrations (2 mol%) and different Yb^{3+} ion concentrations (from 0 to 15 mol%). The inset is the red/green ratio as a function of Yb^{3+} concentrations and the luminescent photograph of Er^{3+}/Yb^{3+} (2/15 mol%) co-doped BiOCl under the excitation of 980 nm at 1.5 W. (For interpretation of the references to color in this figure legend, the reader is referred to the web version of this article.)

(from 0 to 15 mol%) obtained by exciting the samples at 980 nm. It exhibits that an elevated amount of Yb^{3+} dopants increases the intensity of overall UC emissions, especially strongly enhances the red emission after a critical concentration. When the Yb^{3+} ion concentration is over than 2.5 mol%, the red emission becomes dominate and much stronger than other one, thus resulting in a bright red emission output. However, as the Yb^{3+} ions concentration is more than 7.5 mol %, the intensity of overall emissions decreases. According to above results, the UC emission intensity of each band is markedly dependent on the concentration of Er^{3+} and Yb^{3+} ions, and the effect of Yb^{3+} ions is dominant. The optimum Er^{3+}/Yb^{3+} co-doping concentration was found to be 2/7.5 mol % in this system, and the corresponding specimen exhibited a very strong red emission visible to the naked eye when excited by a 980 nm diode laser (inset, Fig. 4(b)).

To investigate the excitation mechanism responsible for the above UC luminescence, the UC spectra were recorded for different excitation laser power values. Fig. 5 presents the violet, green and red UC emission intensities of $Bi_{0.905}Yb_{0.075}Er_{0.02}OCl$ plotted on the logarithmic scale as a function of pump power. For the UC luminescence process, the UC intensity I_{UC} depended on the pumping power I_{Pump} according to the following equation

$$I_{UC} \propto I_{Pump}^{n} \quad (2)$$

In this equation, n is the number of pumping photons required to excite the emitting state. The calculated n values are 3.25, 2.96 and 2.54 for violet emissions, green emission and red emissions, respectively. These results strongly indicate that three-photon processes contribute to both violet and green emissions, suggesting that the $^2H_{11/2}/^4S_{3/2}$ state is populated by nonradiative relaxation (NR) from the higher $^2H_{9/2}$ and $^4G_{11/2}$ states.

However, the n value of the red emission is found to be 2.54, displaying a nearly three-photon process. Moreover, the n values for the red UC luminescence decreased slightly with increasing the Yb^{3+} concentration. The similar phenomenon also appeared in Y_2O_3:Yb^{3+}, Er^{3+} nanocrystals, which may be attributed to the average reduction of the distance between the Yb^{3+} and Er^{3+} ions and the increased ratio of Yb^{3+} ions per Er^{3+} ion, thereby enhancement of the UC rate at the $^4F_{9/2}$ state. [27]. However, such red UC emission was resulted from a two-photon phenomenon. The three-photon UC phenomenon of red emission has been seldom reported, which just was observed at low temperature in a special case [28].

To corroborate the deduction about the three-photon red emission of Er^{3+}, the down-conversion spectra of the $Bi_{0.905}Yb_{0.075}Er_{0.02}OCl$ sample were studied under 380 and 525 nm excitation. Upon excitation with UV radiation (380 nm), Er^{3+} ions in ground state $^4I_{15/2}$ can be excited to the $^4G_{11/2}$ state directly, from which the excited Er^{3+} ions will relax nonradiatively to the $^2H_{11/2}$ and $^4S_{3/2}$ levels and subsequently to the $^4F_{9/2}$ state (Fig. 6). This is probably related to the different local vibration modes of

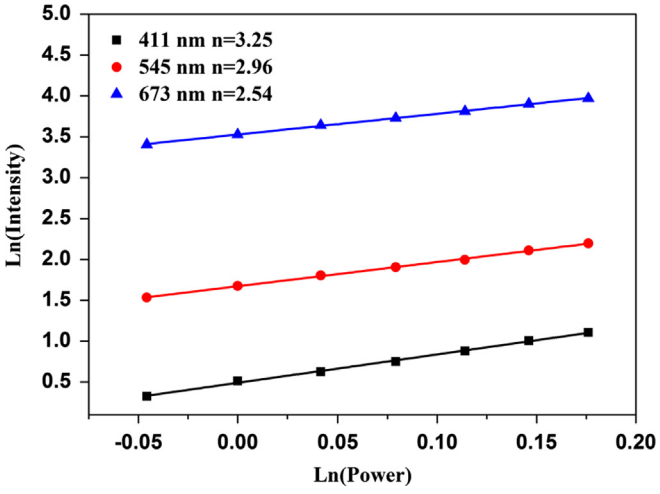

Fig. 5. Power dependence of the UC emission intensities of $Bi_{0.905}Yb_{0.075}Er_{0.02}OCl$ at 411, 545 and 673 nm.

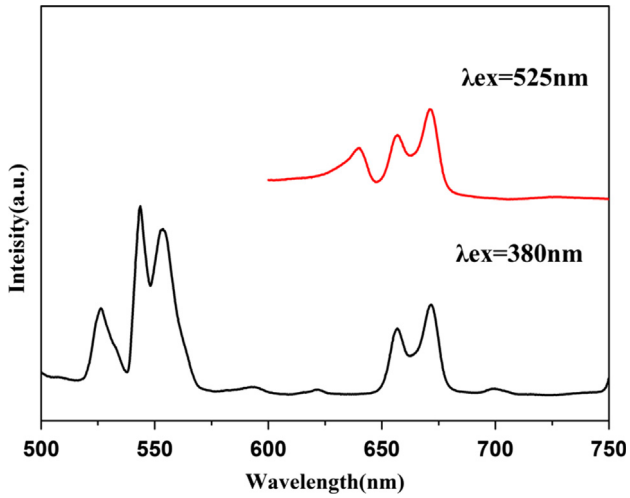

Fig. 6. PL spectrum of $Bi_{0.905}Yb_{0.075}Er_{0.02}OCl$ under 380 and 525 nm excitation.

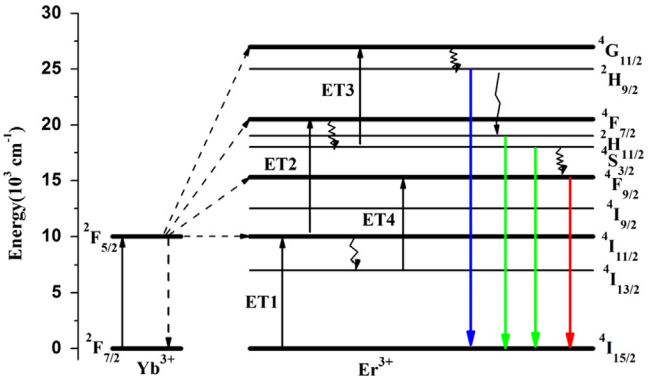

Fig. 7. Energy level diagrams of Er^{3+}/Yb^{3+} co-doped BiOCl and possibly UC mechanisms under 980 nm excitation.

lanthanide impurities. The above result indicates that the populations in high energy states ($^4G_{11/2}$, $^2H_{11/2}$, $^4S_{3/2}$) of Er^{3+} ions can be transformed into the populations in low energy states ($^4F_{9/2}$), confirming that dominated three-photon processes can be included in the red UC emission of Er^{3+} ions. In addition, the PL spectrum under the 525 nm excitation further verify that red and green levels could be populated in the same mode, which provides another evidence for the three-photon red emission of Er^{3+}.

To further recognize the UC mechanisms in the system, the possible UC process were schematically given in the energy level diagrams of Er^{3+} and Yb^{3+}, as shown in Fig. 7. In the Er^{3+}/Yb^{3+} co-doped BiOCl, high-energy levels of Er^{3+} ions can be populated by the energy transfer (ET) from excited Yb^{3+} ions and NR from higher levels of Er^{3+} ions. For the violet and green UC emissions, the routes can be described as

$^4I_{15/2}(Er^{3+})+^2F_{5/2}\ (Yb^{3+})\rightarrow{}^4I_{11/2}(Er^{3+})+^2F_{7/2}\ (Yb^{3+})$ (ET1)
$^4I_{11/2}(Er^{3+})+^2F_{5/2}\ (Yb^{3+})\rightarrow{}^4F_{7/2}(Er^{3+})+^2F_{7/2}\ (Yb^{3+})$ (ET2)
$^4F_{7/2}(Er^{3+})\rightarrow{}^2H_{11/2}/{}^4S_{3/2}(Er^{3+})$ (NR)
$^4S_{3/2}\ (Er^{3+})+^2F_{5/2}\ (Yb^{3+})\rightarrow{}^4G_{11/2}\ (Er^{3+})+^2F_{7/2}$ (Yb^{3+}) (ET3)
Violet emission: $^4G_{11/2}(Er^{3+})\rightarrow{}^2H_{9/2}\ (Er^{3+})$ (NR)
Green emission: $^2H_{9/2}\ (Er^{3+})\rightarrow{}^2H_{11/2}/\ {}^4S_{3/2}(Er^{3+})$ (NR)

For the red emission, the UC process can be considered as the combination of three-photon and two-photon process. The first one is dominated and results from the NR of higher levels excited by a three-photon process, just as described above. The latter one can be expressed as

$^4I_{15/2}(Er^{3+})+^2F_{5/2}\ (Yb^{3+})\rightarrow{}^4I_{11/2}\ (Er^{3+})+^2F_{7/2}\ (Yb^{3+})$ (ET1)
$^4I_{11/2}(Er^{3+})\rightarrow{}^4I_{13/2}(Er^{3+})$ (NR)
$^4I_{13/2}(Er^{3+})+^2F_{5/2}\ (Yb^{3+})\rightarrow{}^4F_{9/2}(Er^{3+})+^2F_{7/2}\ (Yb^{3+})$ (ET4)

4. Conclusions

In conclusion, Er^{3+}/Yb^{3+} co-doped BiOCl poly-crystals were successfully synthesized through a facile solid state method at a moderate temperature. Raman spectra indicate that BiOCl crystal hosts have low phonon energy. Under the 980 nm excitation, UV, violet, green, red and NIR UC emissions from Er^{3+} ion have been observed in Er^{3+}/Yb^{3+} co-doped BiOCl crystals. It was found that the UC emission intensity is markedly dependent on the concentration of Er^{3+} and Yb^{3+} ions and the effect of Yb^{3+} ions is dominant. The laser power dependence of the UC emissions confirmed that three-photon process is responsible for both the violet and green emission, the red emission via a nearly three-photon process in this system. The UC properties of the Er^{3+}/Yb^{3+} co-doped BiOCl poly-crystals indicated that RE doped BiOCl would be low cost, high efficiency UC materials, which can be potentially used in the field color displays, back light, UC lasers, photonics.

Acknowledgments

This work is supported by the Special Program for National Program on Key Basic Research Project of China (No. 2011CB211708), the National Natural Science Foundation of China (No. 61265007), the Society Development Foundation of Yunnan Province (No. 2012FD010) and Measurement and Analysis Foundation of Kunming University of Science and Technology (No. 20130079).

References

[1] F. Auzel, Upconversion and anti-Stokes processes with f and d ions in solids, Chemical Reviews, Columbus 104 (2004) 139–174.
[2] H.X. Mai, Y.W. Zhang, L.D. Sun, C.H. Yan, Highly efficient multicolor up-conversion emissions and their mechanisms of monodisperse $NaYF_4$: Yb, Er core and core/shell-structured nanocrystals, The Journal of Physical Chemistry C 111 (2007) 13721–13729.
[3] S. Schietinger, T. Aichele, H.Q. Wang, T. Nann, O. Benson, Plasmon-enhanced upconversion in single $NaYF_4$: Yb^{3+}/Er^{3+} codoped nanocrystals, Nano Letters 10 (2009) 134–138.
[4] Y. Li, J. Zhang, Y. Luo, X. Zhang, Z. Hao, X. Wang, Color control and white light generation of upconversion luminescence by operating dopant concentrations and pump densities in Yb^{3+}, Er^{3+} and Tm^{3+} tri-doped Lu_2O_3 nanocrystals, Journal of Materials Chemistry 21 (2011) 2895–2900.
[5] S. Cui, H. Chen, H. Zhu, J. Tian, X. Chi, Z. Qian, S. Achilefu, Y. Gu, Amphiphilic chitosan modified upconversion nanoparticles for in vivo photodynamic therapy induced by near-infrared light, Journal of Materials Chemistry 22 (2012) 4861–4873.

[6] J.H. Chung, J.H. Ryu, J.W. Eun, J.H. Lee, S.Y. Lee, T.H. Heo, B. G. Choi, K.B. Shim, Green upconversion luminescence from polycrystalline Yb^{3+}, Er^{3+} Co-doped $CaMoO_4$, Journal of Alloys and Compounds 522 (2012) 30–34.

[7] R. Reiche, L.A.O. Nunes, C.C. Carvalho, Y. Messaddeq, M.A. Aegerter, Blue and green upconversion in Er^{3+}-doped fluoroindate glasses, Solid State Communications 85 (1993) 773–777.

[8] L. An, J. Zhang, M. Liu, S. Wang, Upconversion luminescence of Tm^{3+} and Yb^{3+}-codoped lutetium oxide nanopowders, Journal of Alloys and Compounds 451 (2008) 538–541.

[9] P. Du, Z. Xia, L. Liao, Luminescence properties of $Ca_{0.65}La_{0.35}F_{2.35}$: Yb^{3+}, Er^{3+} with enhanced red emission via upconversion, Materials Research Bulletin 46 (2011) 543–546.

[10] J.C. Boyer, F. Vetrone, L.A. Cuccia, J.A. Capobianco, Synthesis of colloidal upconverting $NaYF_4$ nanocrystals doped with Er^{3+}, Yb^{3+} and Tm^{3+}, Yb^{3+} via thermal decomposition of lanthanide trifluoroacetate precursors, Journal of the American Chemical Society 128 (2006) 7444–7445.

[11] F. Vetrone, J.A. Capobianco, Lanthanide-doped fluoride nanoparticles: luminescence, upconversion, and biological applications, International Journal of Nanotechnology 5 (2008) 1306–1339.

[12] C. Cao, W. Qin, J. Zhang, Y. Wang, P. Zhu, G. Wei, G. Wang, R. Kim, L. Wang, Ultraviolet upconversion emissions of Gd^{3+}, Optics Letters 33 (2008) 857–859.

[13] S. Wu, C. Wang, Y. Cui, T. Wang, B. Huang, X. Zhang, X. Qin, P. Brault, Synthesis and photocatalytic properties of BiOCl nanowire arrays, Materials Letters 64 (2010) 115–118.

[14] X. Zhang, Z. Ai, F. Jia, L. Zhang, Generalized one-pot synthesis, characterization, and photocatalytic activity of hierarchical BiOX (X=Cl, Br, I) nanoplate microspheres, The Journal of Physical Chemistry C 112 (2008) 747–753.

[15] K. Zhang, J. Liang, S. Wang, J. Liu, K. Ren, X. Zheng, H. Luo, Y. Peng, X. Zou, X. Bo, BiOCl sub-microcrystals induced by citric acid and their high photocatalytic activities, Crystal Growth and Design 12 (2012) 793–803.

[16] Z. Deng, D. Chen, B. Peng, F. Tang, From bulk metal Bi to two-dimensional well-crystallized BiOX (X=Cl, Br) micro-and nanostructures: synthesis and characterization, Crystal Growth and Design 8 (2008) 2995–3003.

[17] Z. Deng, F. Tang, A.J. Muscat, Strong blue photoluminescence from single-crystalline bismuth oxychloride nanoplates, Nanotechnology 19 (2008) 295705–295710.

[18] S. Cao, C. Guo, Y. Lv, Y. Guo, Q. Liu, A novel BiOCl film with flowerlike hierarchical structures and its optical properties, Nanotechnology 20 (2009) 275702–276708.

[19] A. Patra, C.S. Friend, R. Kapoor, P.N. Prasad, Upconversion in Er^{3+}: ZrO_2 nanocrystals, The Journal of Physical Chemistry B 106 (2002) 1909–1912.

[20] O. Meza, L.A. Diaz-Torres, P. Salas, E. De la Rosa, D. Solis, Color tunability of the upconversion emission in Er–Yb doped the wide band gap nanophosphors ZrO_2 and Y_2O_3, Materials Science and Engineering: B 174 (2010) 177–181.

[21] C. de Mello Donegá, H. Lambaerts, A. Meijerink, G. Blasse, The vibronic spectroscopy of Pr^{3+} in YOCl and LaOCl, Journal of Physics and Chemistry of Solids 54 (1993) 873–881.

[22] Y. Li, X. Wei, M. Yin, Synthesis and upconversion luminescent properties of Er^{3+} doped and Er^{3+}–Yb^{3+} codoped GdOCl powders, Journal of Alloys and Compounds 509 (2011) 9865–9868.

[23] L. Zhao, X. Zhang, C. Fan, Z. Liang, P. Han, First-principles study on the structural, electronic and optical properties of BiOX(X=Cl, Br, I) crystals, Physica B: Condensed Matter 407 (2012) 3364–3370.

[24] W.L. Huang, Q. Zhu, Electronic structures of relaxed BiOX (X=F, Cl, Br, I) photocatalysts, Computational Materials Science 43 (2008) 1101–1108.

[25] L. Zhang, W.Z. Wang, S.M. Sun, Z.J. Zhang, J.H. Xu, J. Ren, Photocatalytic activity of Er^{3+}, Yb^{3+} doped Bi_5O_7I, Catalysis Communications 26 (2012) 88–92.

[26] J. Zhang, S. Wang, T. Rong, L. Chen, Upconversion luminescence in Er^{3+} doped and Yb^{3+}/Er^{3+} codoped yttria nanocrystalline powders, Journal of the American Ceramic Society 87 (2004) 1072–1075.

[27] G.Y. Chen, Y. Liu, Z.G. Zhang, B. Aghahadi, G. Somesfalean, Q. Sun, F. P. Wang, Four-photon upconversion induced by infrared diode laser excitation in rare-earth-ion-doped Y_2O_3 nanocrystals, Chemical Physics Letters 448 (2007) 127–131.

[28] K. Zheng, L. Wang, D. Zhang, D. Zhao, W. Qin, Power switched multiphoton upconversion emissions of Er^{3+} in Yb^{3+}/Er^{3+} codoped beta-$NaYF_4$ microcrystals induced by 980 nm excitation, Optics Express 18 (2010) 2934–2939.